Received: 4 August 2021 | Revised: 27 September 2021 | Accepted: 28 September 2021

DOI: 10.1096/fj.202101232RR

THE FASEB JOURNAL

RESEARCH ARTICLE

Orthogonal ubiquitin transfer reveals human papillomavirus E6 downregulates nuclear transport to disarm interferon-γ dependent apoptosis of cervical cancer cells

Yiyang Wang[1,2] | Ruochuan Liu[2] | Jia Liao[1] | Lucen Jiang[3] | Geon H. Jeong[2] | Li Zhou[2] | Monica Polite[2] | Duc Duong[4] | Nicholas T. Seyfried[5] | Huadong Wang[1] | Hiroaki Kiyokawa[6] | Jun Yin[2]

[1]Department of Pathophysiology, School of Medicine, Jinan University, Guangzhou, China

[2]Department of Chemistry and Center for Diagnostics and Therapeutics, Georgia State University, Atlanta, Georgia, USA

[3]Department of Pathology, The Third Affiliated Hospital of Southern Medical University, Guangzhou, China

[4]Integrated Proteomics Core, Emory University, Atlanta, Georgia, USA

[5]Department of Biochemistry, Emory University School of Medicine, Atlanta, Georgia, USA

[6]Department of Pharmacology, Northwestern University, Chicago, Illinois, USA

Correspondence

Huadong Wang, Department of Pathophysiology, School of Medicine, Jinan University, Guangzhou, China.
Email: twhd@jnu.edu.cn

Hiroaki Kiyokawa, Department of Pharmacology, Northwestern University, Chicago, IL 60611, USA.
Email: kiyokawa@northwestern.edu

Jun Yin, Department of Chemistry and Center for Diagnostics and Therapeutics, Georgia State University, Atlanta, GA 30303, USA.
Email: junyin@gsu.edu

Funding information

National Science Foundation (NSF), Grant/Award Number: 1710460 and 2109051; Fundamental Research Funds for the Central Universities of China, Grant/Award Number: 21619329; HHS | National Institutes of Health (NIH), Grant/Award Number: R01GM104498

Abstract

The E6 protein of the human papillomavirus (HPV) underpins important protein interaction networks between the virus and host to promote viral infection. Through its interaction with E6AP, a host E3 ubiquitin (UB) ligase, E6 stirs the protein ubiquitination pathways toward the oncogenic transformation of the infected cells. For a systematic measurement of E6 reprogramming of the substrate pool of E6AP, we performed a proteomic screen based on "orthogonal UB transfer (OUT)" that allowed us to identify the ubiquitination targets of E6AP dependent on the E6 protein of HPV-16, a high-risk viral subtype for the development of cervical cancer. The OUT screen identified more than 200 potential substrates of the E6-E6AP pair based on the transfer of UB from E6AP to the substrate proteins. Among them, we verified that E6 would induce E6AP-catalyzed ubiquitination of importin proteins KPNA1-3, protein phosphatase PGAM5, and arginine methyltransferases CARM1 to trigger their degradation by the proteasome. We further found that E6 could significantly reduce the cellular level of KPNA1 that resulted in the suppression of nuclear transport of phosphorylated STAT1 and the inhibition of interferon-γ-induced apoptosis in cervical cancer cells. Overall, our

Abbreviations: DUB, deubiquitinating enzymes; E1, E1 ubiqutin-activating enzyme; E2, E2 ubiquitin-conjugating enzyme; E3, E3 ubiquitin ligase; E6AP, E6-associated protein; HECT, homologous to the E6AP carboxyl terminus (HECT) domain family; HPV, human papillomavirus; IFN, interferons; OUT, orthogonal ubiquitin transfer; UB, ubiquitin.

Yiyang Wang and Ruochuan Liu contributed equally to this study.

work demonstrates OUT as a powerful proteomic platform to probe the interaction of E6 and host cells through protein ubiquitination and reveals a new role of E6 in down-regulating nuclear transport proteins to attenuate tumor-suppressive signaling.

KEYWORDS

apoptosis, E6, E6AP, nuclear transport, orthogonal ubiquitin transfer

1 | INTRODUCTION

Human papillomaviruses (HPVs) constitute a diverse family of small double-stranded DNA viruses that are penetrating factors for cancer development in the anogenital tract and cutaneous tissues.[1,2] Among various subtypes of HPV, HPV-16 and HPV-18 are of high risk and causative for 80% of cervical cancers worldwide.[3,4] Upon virus entry into the epithelial cells, the HPV viral DNA is incorporated into the host cell genome, and the expression of the early viral genes E6 and E7 stimulates proliferation of the infected cells and sets them on a path for oncogenic transformation.[5–7] The manipulation of the protein ubiquitination pathways by the E6 and E7 oncoproteins are determining factors of host cell transformation.[8] E6 hijacks the E6-associated protein (E6AP), an E3 ubiquitin (UB) ligase in the host cell, to ubiquitinate p53 and promote its degradation by the proteasome.[9–11] The attenuated p53 activity would enhance the survival of the infected cells and their progression toward tumorigenesis. E7 functions as a substrate adaptor that would redirect Cullin E3 UB ligase Cul2 to ubiquitinate pRb, a cell cycle regulator, and induces its proteasomal degradation.[12,13] This drives the G1 to S-phase transition of the cell cycle in favor of cell proliferation and virus amplification.

Besides the well-established mechanisms of E6 and E7 in coercing the host ubiquitin-proteasome systems for cancer development, other targets of E6 in the host cells have been unraveled and suggest multifaceted roles of the viral oncoprotein in HPV-induced cancers.[14–16] The E6-E6AP pair has been found to ubiquitinate the proapoptotic protein Bak,[17,18] the tumor suppressors Scribble, Dlg, and PTPH1,[19–21] and the transcription factors myc and NFX1-91 and induce their degradation.[22–24] Destabilization of NFX1-91 activates the hTERT promoter and enhances the expression of telomerase in HPV infected cells to facilitate unrestricted proliferation.[22,23] Besides E6AP, E6 may pair with other E3s such as EDD1 to degrade acetyltransferase TIP60.[25,26] Other host cell proteins such as PATJ, MAGI-3, DLG1, and Scribble could be associated with E6 through a PDZ domain and induced for degradation independent of E6AP.[27–29] It also has been shown that E6 association does not necessarily lead to the destabilization of the interacting proteins. For example, E6 suppresses enzymatic activities of the histone methyltransferases CARM1, PRMT1, and SET7 by altering their expression profile,[30] and E6 binding to the Notch transcription factor inhibits the activation of Notch-targeting genes.[31] These findings denote that E6 may orchestrate diverse pathways in the host cell to facilitate HPV infection and subsequent cancer development.

We recently developed a method to screen the ubiquitination substrates of E6AP by building an OUT cascade, in which an engineered UB (xUB) could be exclusively used by E6AP to label its substrate proteins for their identification by proteomics.[32] The construction of OUT is based on the engineering of xUB bearing the R42E and R72E mutations (xUB), so that it is rejected by the wild type (wt) UB transfer cascades of E1–E2–E3 enzymes but would instead be delivered by an engineered xE1–xE2–xE3 cascade to the direct substrate of a specific E3 ("x" designates the engineered UB transferring enzymes sharing no cross activity with the wt enzymes).[33–35] We engineered Uba1 (E1), UbxH7 (E2), and E6AP (E3) to generate orthogonal xUB-xUba1, xUba1-xUbcH7, and xUbcH7-xE6AP pairs, so xUB could be transferred through the OUT cascade to the direct substrates of E6AP in the cell.[32,33] We expressed the OUT cascade in the cell with 6×His-biotin-tagged xUB (HBT-xUB) to allow xUB conjugation with the E6AP substrates, and then we carried out tandem purification of xUB-conjugated proteins and revealed their identities by proteomics. In this report, we took advantage of the OUT cascade we engineered for E6AP to profile its substrates in the presence and absence of E6 from HPV16 (Figure 1A). By identifying new E6AP substrates accompanying E6 expression in the cell, we found numerous potential targets of E6-E6AP and confirmed the roles of E6 in enhancing the ubiquitination of protein methyltransferases CARM1 and PGAM5, and nuclear transport proteins KPNA1-3 by E6AP.

KPNA1-3 are adaptor proteins of the importin α (karyopherin subunit α) family, which pair with nuclear transport receptor KPNB1 (importin β or karyopherin β1) for shuttling diverse cargo proteins from the cytoplasm to

the nucleus through the nuclear pore complex (NPC).[36] Numerous transcription factors such as STAT1-3 and NF-κB rely on KPNAs for nuclear transport, and once in the nucleus, they would activate host response to oncogenic viral infection to incite local immunity.[37–39] We thus hypothesize that E6AP activation by HPV E6 would enhance the ubiquitination and degradation of KPNA proteins and suppress the transport of antiviral transcription factors into the nucleus, and this would promote the survival of host cells undergoing pro-tumorigenic transformation. Indeed, many KPNA cargo proteins are involved in host cell response to viral infection. KPNA1 (importin α5) is critical for nuclear transport of STAT1 and STAT2, two transcription factors activated by the JAK1 and TYK2 kinases as a part of antiviral response stimulated by interferons (IFNs).[40–42] KPNA2 (importin α1) is involved in the trafficking of NF-κB to the nucleus,[43,44] and KPNA3 (importin α4) mediates nuclear localization of p53 and RanBP3.[45,46] Our data suggest that E6 of HPV16 promotes E6AP-mediated ubiquitination and degradation of KPNA1-3, and E6-induced KPNA1 destabilization leads to the suppression of nuclear transport of STAT1 and inhibition of apoptotic response mediated by IFN-γ.

2 | MATERIALS AND METHODS

2.1 | Materials and cell culture

BL21 (DE3) pLysS chemical competent cells were obtained from Invitrogen. XL1-Blue cells were from Agilent Technologies (Santa Clara, California, USA). pET-15b and pET-28a plasmids for protein expression were from Novagen. The plasmids of pLenti-E6 (#37445), pCMVTNT-T7-KPNA1 (#26677), pCMVTNT-T7-KPNA2 (#26678), pCDNA-CARM1 (#81118), pNIC28-Bsa4-PGAM5 (#38976), and pCMVTNT-T7-KPNA3 (#26679) were from Addgene. Expression plasmids for the OUT components of E6AP were constructed in a previous study.[32] Anti-HA antibody (sc-7392), anti-Myc antibody (sc-40), anti-tubulin antibody (sc-23948), anti-V5 antibody (sc-271944), anti-ubiquitin antibody (sc-8017), anti-CARM1 antibody (sc-390656), anti-KPNA1 antibody (sc-101292), anti-KPNA2 antibody (sc-55538), anti-KPNA3 antibody (sc-514101), and anti-PGAM5 antibody (sc-161156) were purchased from Santa Cruz Biotechnology (Dallas, TX). Anti-Lamin B antibody (#13435s), anti-GAPDH antibody (#2118s), anti-pSTAT1 antibody (#9177s), anti-STAT1 antibody (#9172), anti-cleaved caspase-3 antibody (#9661S), anti-cleaved caspase-8 antibody (#9748), anti-cleaved caspase-9 antibody (#20750), anti-caspase3 antibody (#9662), anti-caspase 8 antibody (#4790), anti-caspase 9 antibody (#9508), anti-Bim antibody (#2933s), anti-FAS antibody (#8023), and anti-iNOS antibody (#39898) were purchased from Cell Signaling Technology (Danvers, MA). Goat anti-rabbit IgG antibody (#31462) and goat anti-mouse IgG antibody (#31438) was obtained from Thermo Fisher Scientific (Logan, UT). Anti-flag (M2) antibody (F3165) was purchased from Sigma-Aldrich (St Louis, MO). HPV-16 E6 protein was from Boston Biochem (Cambridge, MA). Nuclear and cytoplasmic extraction reagents (#78833) as well as SuperSignal® West Pico Chemiluminescent Substrate (#34580) were purchased from Thermo Fisher Scientific (Logan, UT). HEK293, HeLa and C33A cells were from American Tissue Culture Collection (ATCC). HEK293 and HeLa cell were cultured in high-glucose Dulbecco's modified Eagles medium (DMEM) (Life Technologies, Carlsbad, CA, USA, 11965092) with 10% (v/v) fetal bovine serum (FBS) (Life Technologies, 11965092). C33A cells were cultured in minimum Eagle's medium (MEM) with 10% FBS.

2.2 | Tandem affinity purification of xUB-conjugated proteins

HEK293 cells expressing the OUT cascades of E6AP including Flag-xUba1, V5-xUbcH7, and Myc-xE6AP were constructed previously.[32] The stable cells of the E6AP OUT cascade were transiently transfected with pLenti-HBT-xUB and pLenti-HA-E6 plasmids and cultured for 48 h. Tandem purification of HBT-xUB-conjugated proteins was performed as previously described.[32] Briefly, cells were treated with 10 μM MG132 (American Peptide, Sunnyvale, CA) for 4 h at 37°C to inhibit proteasome activity. The cells were then washed twice with cold PBS and harvested by a cell scraper with buffer A (8 M urea, 300 mM NaCl, 50 mM Tris, 50 mM NaH_2PO_4, 0.5% NP-40, 1 mM phenylmethylsulfonyl fluoride, and benzonase [125 U/ml] [pH 8.0]). For Ni-NTA purification, cell lysates were centrifuged at 15,000×*g* for 30 min at room temperature. About 60 mg of cellular protein was collected for tandem purification. For each 1 mg of protein lysate, 35 μl of Ni^{2+} Sepharose beads (GE Healthcare) was added to the clarified supernatant. After incubation overnight at room temperature in buffer A with 10 mM imidazole on a rocking platform, Ni^{2+} Sepharose beads were pelleted by centrifugation at 100×*g* for 3 min and washed sequentially with a 20-bead volume of buffer A (pH 8.0), buffer A (pH 6.3), and buffer A (pH 6.3) with 10 mM imidazole. After washing the beads, proteins were eluted twice with a 5-bead volume of buffer B (8 M urea, 200 mM NaCl, 50 mM Na_2HPO_4, 2% SDS, 10 mM EDTA, 100 mM Tris, and 250 mM imidazole [pH 4.3]). For streptavidin purification, the elution solution was adjusted to pH 8.0.

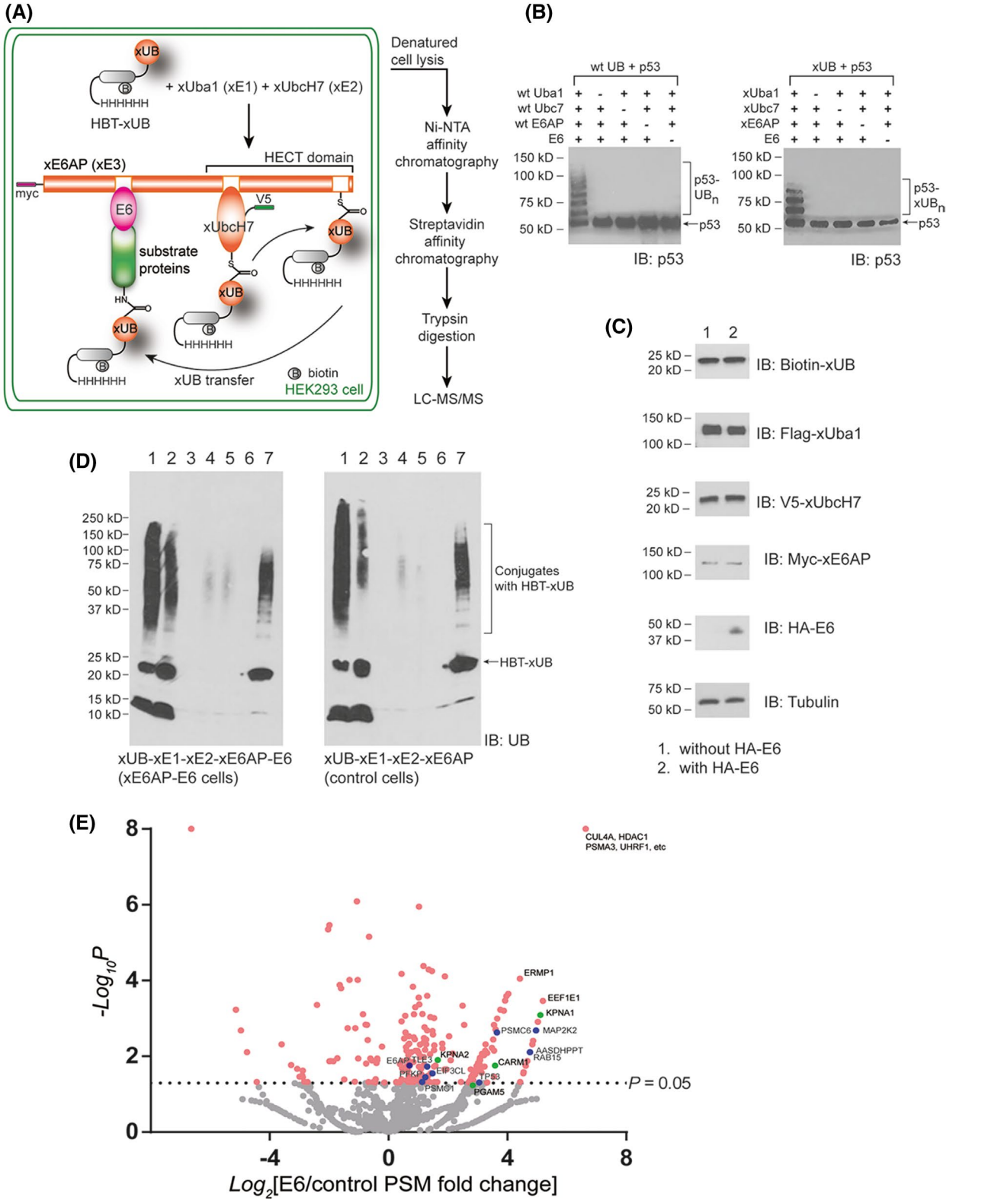

For streptavidin binding, 50 µl of streptavidin sepharose beads (Thermo Fisher Scientific, Logan, UT) were added to the eluate to bind HBT-xUB-conjugated proteins. After incubation on a rocking platform overnight at room temperature, streptavidin beads were pelleted and washed sequentially with buffer C (8 M urea, 200 mM NaCl, 2% SDS, and 100 mM Tris [pH 8.0]), buffer D (8 M urea, 1.2 M NaCl, 0.2% SDS, 100 mM Tris, 10% EtOH, and 10% isopropanol [pH 8.0]), and buffer E (8 M urea and 100 mM NH_4HCO_3 [pH 8.0]).

FIGURE 1 Using the orthogonal UB transfer (OUT) cascade of E6AP to identify E6AP substrates stirred by E6 in HEK293 cells. (A) Scheme for expressing HBT-xUB and the xUba1-xUbcH7-xE6AP OUT cascade in the cell with the co-expression of E6 of HPV16. Proteins dependent on E6 for ubiquitination by E6AP were conjugated with HBT-xUB and purified under denaturing conditions by tandem affinity chromatography with Ni-NTA and streptavidin resins. Proteins bound to the streptavidin resin were digested by trypsin and identified by MS-based proteomics. (B) Verifying E6-mediated p53 ubiquitination in vitro with wt E6AP and the OUT cascade of E6AP. In the presence of E6, xE6AP can transfer xUB to p53 at a similar efficiency as wt E6AP in transferring wt UB to p53. (C) Expression of HBT-xUB, the OUT cascade enzymes, and the E6 protein in HEK293 cells (xE6AP-E6 cells) and the expression of HBT-xUB and the OUT cascade enzymes in cells without E6 coexpression (control cells). (D) Tandem purification of xUB-conjugated proteins from the lysates of xE6AP-E6 cells and control cells. (1) Cell lysates before Ni-NTA binding; (2) flow-through of the cell lysates after Ni-NTA binding; (3) wash of the Ni-NTA beads; (4) elution from the Ni-NTA beads; (5) flow-through from the streptavidin beads; (6) wash of the streptavidin beads; (7) proteins bound to the streptavidin beads. (E) Volcano plot of the proteins identified by the E6AP OUT cascade with the co-expression of E6. The average fold changes of PSM numbers ($-\text{Log}_2$[E6/control PSM fold change]) of proteins from three repeats of tandem purifications from cells expressing the OUT cascade of E6AP with and without the co-expression of E6 were plotted against the p values ($-\text{Log}_{10}p$) of the corresponding proteins in the volcano plot. Student's t-test was used to generate the p values for the plot (Table S3). Red dots designate proteins with $p < .05$ ($-\text{Log}_{10}p > 1.3$). Green dots designate proteins characterized as the substrates of the E6-E6AP pair in this study, and blue dots designate proteins reported as E6 interactors in the literature

2.3 | Sample digestion and LC-MS/MS analysis

After tandem purification, the streptavidin beads were spun down and washed to remove the residual urea. The HBT-xUB conjugated proteins bound to the beads were digested by LysC and trypsin following an established protocol.[32] For analysis by mass spectrometry, each sample was reconstituted in 20 μl of loading buffer (0.1% formic acid) and 4 μl was loaded onto a 25 cm × 75 μm ID column in-house packed with 1.9 μm Dr. Maisch C18 beads. Elution started at 3% buffer B (acetonitrile with 0.1% formic acid) and ended with 30% B over 105 min. This was followed by a 20-min increase to 60% B and 15-min flush at 99% B. The Fusion orbitrap mass spectrometer at the Emory Integrated Proteomics Core (Thermo Fisher Scientific, Logan, UT) was operated at top speed for 3 s cycles. Each cycle consisted of 1 survey scan (120,000 resolution, 400–1,500 m/z range, 50 ms max injection time, and 200,000 automatic gain control) and a round of tandem MS higher energy collision dissociation scans (charges 2 to 7, 1.6 m/z isolation window, 30% normalized collision energy, 35 ms max injection time, and 10,000 automatic gain control) collected in the ion trap. Dynamic exclusion was set to 30 s.

2.4 | Analysis of the proteomics data

All spectra files were searched using Thermo's Proteome Discoverer Suite (version 2.1.1.21) against a Human uniprot database (downloaded on March 2015, 90,300 target sequences). Search parameters included fully tryptic enzyme, maximum of two miscleavages, precursor tolerance of 20 ppm, product ion tolerance of 0.6 Da, dynamic modifications for methione oxidation (+15.995 Da), asparagine and glutamine deamidation (+0.984 Da), lysine ubiquitination (+114.04293 Da), and static modification of cysteine carbamidomethyl (+57.021 Da). Scored spectra were filtered to percolator to a peptide and PSM level of 0.01 fdr. A Student's t-test was used to generate the p values for the volcano plot. The PSM values for the three sets were median normalized for the p value calculation to account for signal variation across the batches because the experiments were run months apart. The values of $\log_2$ fold change were calculated based on the averages of the original PSM values.

2.5 | Protein expression and purification

BL21 (DE3) pLysS chemical competent *Escherichia coli* cells were transformed with the pET expression plasmids (Invitrogen) and plated on the LB-agar plates with appropriate antibiotics. Protein expression and purification followed the protocol provided by the vendor of the pET expression system (Novagen) and the Ni-NTA agarose resin (Qiagen). Purification of GST-tagged proteins from *E. coli* transformed with the pGEX vector followed the standard protocol for protein purification with glutathione-agarose beads (Thermo Fisher Scientific).

2.6 | In vitro ubiquitination assay

cDNAs of the potential substrates, KPNA1, KPNA2, KPNA3, and PGAM5 were cloned into the pET vector for protein expression. CARM1 protein was purchased from Creative Biomart. To assay ubiquitination by E6AP and E6, each substrate protein (5 μM) was incubated with 1 μM wt Uba1, 5 μM wt UbcH7, 50 μM wt UB, 10 μM wt E6AP, and 0.3 μM E6 in TBS supplemented with 10 mM

$MgCl_2$ and 1.5 mM ATP for 2 h at 30°C. Ubiquitination of those substrates was analyzed by Western blotting probed with either substrate-specific antibodies or antibodies against the GST tag fused to the substrates.

2.7 | Co-immunoprecipitation

Transfections of pLenti-Myc-wtE6AP and pLenti-E6 into the HEK293 cells were conducted with the Lipofectamine 2000 according to the manufacturer's protocol. To immunoprecipitate substrate proteins, cells were treated with 10 μM MG132 for 90 min at 48 h post-transfection. HEK293 cells (80%–90%) confluent monolayer in 75 cm^2 cell culture flask expressing control plasmid, pLenti-E6AP, pLenti-E6, and pLenti-E6AP + pLenti-E6 were washed twice with ice-cold PBS. One microliter ice-cold RIPA buffer was added to cell monolayer and incubated with the cells at 4°C for 10 min. The cell lysate was transferred to a 1.5 ml tube. The cell debris was pelleted by centrifugation at 13,000 rpm. for 20 min at 4°C, and the supernatant was transferred to a 1.5 ml centrifuge tube and pre-cleared by adding 1.0 μg of the appropriate control IgG (normal mouse or rabbit IgG corresponding to the host species of the primary antibody). After that, 20 μl of re-suspended Protein A/G PLUS-agarose beads were added to the supernatant, and the incubation was continued for 30 min at 4°C. The beads were pelleted by centrifugation at 350×*g* for 5 min at 4°C. From the cleared cell lysate, a volume containing 2 mg total protein was transferred to a new tube and 30 μl (6 μg) of primary antibody against a specific substrate protein were added, and incubation was continued for 1 h at 4°C. After incubation, 50 μl of the re-suspended volume of Protein A/G PLUS-Agarose was added. The tubes were capped and incubate at 4°C on a rocking platform overnight. The agarose beads were pelleted by centrifugation at 350×*g* for 5 min at 4°C. The beads were then washed 4 times, each time with 1.0 ml PBS. After the final wash, the beads were re-suspended in 40 μl 1 × Laemmli buffer with BME. The samples were boiled for 5 min and analyzed by SDS-PAGE and Western blotting probed with an antibody against UB.

2.8 | Immunofluorescence staining

HEK293 cells with/without pLenti-E6AP or pLenti-E6 transfection after treatment with 100 ng/ml IFN-γ for 30 min were fixed with 4% formalin solution. The cells were then treated with 0.1% Triton X-100 in PBS to make intracellular protein binding sites more accessible for the antibodies. After 3-time washing with PBS for 5 min each time, the cells were blocked in PBS with 1% BSA, following an incubation with 1:100 dilution of antibodies against KPNA1 and pSTAT1 at 4°C overnight. The cells were then incubated with the secondary antibodies using Alexa Fluor 647-labelled donkey antibody against rabbit IgG (A32733, Thermo Fisher Scientific, Logan, UT) for pSTAT1 detection and Alexa Fluor 488-labelled goat antibody against mouse IgG (A32723, Thermo Fisher Scientific, Logan, UT) for KPNA1 detection. The secondary antibodies were diluted 300-fold and incubated with the cells for 1 h. The cells were then washed three times with PBS with 5-min incubation in the PBS buffer between the washes. Finally, the cells were incubated with 1:200 dilution of 4,6-diamidino-2-phenylindole (DAPI) for 15 min and observed with laser confocal microscopy.

2.9 | Western blotting analysis

Cytosolic and nuclear proteins were harvested from HEK293, HeLa, or C33A cells, and protein concentrations of the cell lysates were determined. The levels of specific proteins were determined by Western blotting assay as previously described.[32] The following primary antibodies were used: anti-HA, anti-Myc, anti-tubulin, anti-ubiquitin, anti-CARM1, anti-KPNA1/2/3, anti-PGAM5, anti-Lamin B, anti-GAPDH, anti-pSTAT1, anti-STAT1, anti-cleaved caspase-3/8/9, anti-caspase3/8/9, anti-Bim, anti-FAS, and anti-iNOS. Goat anti-rabbit IgG antibody and goat anti-mouse IgG antibody were used as secondary antibody. Images were captured with a Gel Logic 2200 system for densitometry. Blots from at least three independent experiments were used for quantification purposes and representative data were shown. The Image J software, an open-source image processing program, was used to quantify blots (mean normalized net intensities ± S.E.).

2.10 | Terminal deoxynucleotidyl transferase-mediated dUTP nick-end-labeling (TUNEL) assay

Apoptosis of C33A cells was assessed by the TUNEL assay using the in-situ apoptosis detection kit (Roche, CA, USA). C33A cells were treated with 100 ng/ml IFN-γ for 12 h after pLenti-E6AP or pLenti-E6 transfection. After fixation by 4% formalin solution and permeabilization with Triton X-100, the C33A cells were incubated with TUNEL reaction mixture at 37°C for 1 h in the dark. The cells were rinsed with PBS, then incubated with 1:200 dilution of DAPI for 15 min and observed with a fluorescence microscope. Apoptotic cells were counted in five

randomly selected fields per sample and a mean of five images per chamber was calculated. Images from at least three independent experiments were used for quantification purposes and representative data were shown.

2.11 | Statistical analysis

Mean densitometry and all other quantitative data were presented as mean ± standard error of the mean (SEM). Comparison among multiple groups was made using one-way ANOVA followed by the Student–Newman–Keuls test or an unpaired Student *t*-test. The differences were considered statistically significant at the level of $p < .05$. The SPSS (version 13.0; SPSS Inc., Chicago, IL, USA) software was used to analyze the data.

3 | RESULTS

3.1 | Identifying the substrates of the E6-E6AP pair by OUT

The development of the OUT cascade of E6AP prompted us to compare the substrate profiles of the E3 in the absence and presence of E6 expression to unravel how E6 stirs the substrate specificity of E6AP[32] (Figure 1A). The mutations we put in the HECT domain of E6AP for constructing the xUbcH7-xE6AP pair are within the loop of ^{651}DDMMIT^{656} in the middle of the HECT domain and would not interfere with the binding of E6 with the ^{386}LQELLGEE^{393} motif in E6AP that is more than 100 residues upstream of the N-terminus of the HECT domain.[47,48] We thus posited that E6 would bind to xE6AP with HECT domain mutations in the same mode as it binds to wt E6AP to mediate UB transfer to E6-specific substrates. We confirmed the in vitro transfer of xUB to p53 through the OUT cascade of E6AP and the E6 protein of the HPV16, demonstrating E6 functions normally with the OUT cascade of E6AP (Figure 1B). We then transiently transfected the expression vectors of HBT-xUB and E6 into HEK293 cells stably expressing the E6AP OUT cascade, to initiate the transfer of xUB through the E6AP OUT cascade and E6 to the substrate proteins (Figure 1A). In parallel, we transiently transfected the HBT-xUB vector into the HEK293 cells stably expressing the E6AP OUT cascade to initiate xUB transfer to the E6AP substrates in the absence of E6. Expression of each component of the OUT cascade such as HBT-xUB, Flag-xUba1, V5-xUbcH7, and myc-xE6AP were confirmed by Western blot analysis of the cell lysates, using streptavidin or specific antibodies against the affinity tags fused to the OUT components (Figure 1C). Expression of E6 in cells transfected with the E6 plasmid was also confirmed by probing the Western blots with an anti-E6 antibody.

We purified xUB-conjugated proteins from two cultures of cells with and without E6 in buffers containing 8 M of urea to minimize non-specific association of proteins with the Ni-NTA or the streptavidin matrix (Figure 1D). Proteins tandemly purified from cells expressing the E6AP OUT cascades and E6 (xE6AP-E6 cells) and cells expressing the E6AP OUT cascade only (control cells) were digested by trypsin and the peptide fragments were identified by LC-MS/MS. We repeated the procedure of sample preparation and purification three times, and each time we compared the peptide spectrum numbers (PSMs) of the proteins and filtered out the proteins with 2-fold or higher PSM ratios between the xE6AP-E6 cells and control cells. We then compared the filtered list of the three biological/technical replicates and identified proteins that showed 2-fold or higher PSM ratios in at least two out of three repeats.

In total, we identified 240 candidate proteins passing our filtering criterion and these are the potential E6AP substrates stirred by the E6 protein for ubiquitination reaction catalyzed by E6AP (Table S1). Among them, we found p53 which is the classical target of the E6-E6AP pair.[10] We also found a number of proteins that were previously identified to interact with E6, including AADHPPT, EIF3CL, KPNA2, p53, ZNF326, MTA2, and PFKP which were demonstrated to bind to E6 by affinity purification,[49,50] KPNA2, MAP2K2, Rab15, and CARM1 identified by a screen based on luciferase complementation assay,[51] and MCM7 found in yeast two-hybrid screens.[52] The OUT screen of the E6-E6AP pair also identified numerous substrates of the protein ubiquitination and degradation pathways that were reported to interact with E6, including deubiquitinating enzymes (DUB) USP7 and USP39, Cullin E3 adaptor TLE3, and proteasome components PSMC1 and PSMC6.[49,51] We also compared the list of potential substrates of the E6-E6AP pair from this study with the list of E6AP substrates without E6 expression identified by the OUT screen from our earlier study,[32] and found 26 substrates that appeared in both lists (Table S2). These substrates are likely to be recognized primarily by the E6AP enzyme rather than interacting with E6. Their appearance in the E6-E6AP substrate list suggests that E6 could enhance the ubiquitination of these proteins catalyzed by E6AP. We analyzed the proteomics data by volcano plot to identify potential substrates of the E6-E6AP pair that showed significant enrichment from cells co-expressing E6 with the E6AP OUT cascade over the cells without the E6 expression (Figure 1E and Table S3). The volcano plot analysis identified 244 proteins in the zone of $p < .05$ ($-\log_{10}p > 1.3$) and PSM ratio between E6 expressed and non-expressed cells greater than 2 ($-\log_2$[E6/control PSM

fold change] > 1). Among them, we found known interactors of E6, including AASDHPPT, EIF3CL, KPNA2, MAP2K2, PKFP, PSMC1, PSMC6, Rab15, and TLE3. p53, the classical substrates of the E6-E6AP pair, has a *p* value of .057, close to the .05 mark of the *p* value.

3.2 | Verifying the potential substrates of the E6-E6AP pair identified by OUT

We chose to verify Ser/Thr protein phosphatase PGAM5, arginine methyltransferases CARM1, and nuclear transporting proteins KPNA1-3 from the list of OUT profiles since these proteins may have potential roles in regulating the host antiviral response.[30,53,54] KPNA1, KPNA2, and CARM1 have a *p* value less than .05 for their consistent enrichment from the cells with the co-expression of E6 and the OUT cascade of E6AP (Figure 1E and Table S3). PGAM5 has a *p* value of .06, close to the .05 mark. KPNA3 has a higher *p* value of .71, but since it is in the importin α family with KPNA1 and KPNA2, we also verified its ubiquitination by the E6-E6AP pair. We first expressed and purified the proteins from *E. coli* and tested if they would be ubiquitinated in vitro by the E6-E6AP pair. We found PGAM5 could be polyubiquitinated by the E6-E6AP pair and the ubiquitination reaction was dependent on the presence of E6 (Figure 2A). CARM1 had enhanced polyubiquitination with the E6-E6AP pair comparing to the reaction with E6AP alone (Figure 2B). Polyubiquitination of KPNA1-3 also depended on the presence of E6-E6AP pair. KPNA1 and KPNA2 showed strong ubiquitination in the in vitro reactions while KPNA3 exhibited weak ubiquitination by E6-E6AP (Figure 2C–E).

We then tested if E6 expression would enhance E6AP-mediated ubiquitination of the substrates in HEK293 cells. We expressed E6AP and E6 either separately or together in HEK293 cells by transient transfection. For this experiment, we used the V42L mutant of HPV16 E6, instead of wt E6, since it has been reported that the mutation would remove a splicing site in the messenger RNA of E6 and enhance its expression.[50,55,56] We treated the transfected cells with the proteasome inhibitor MG132 for 4 h prior to

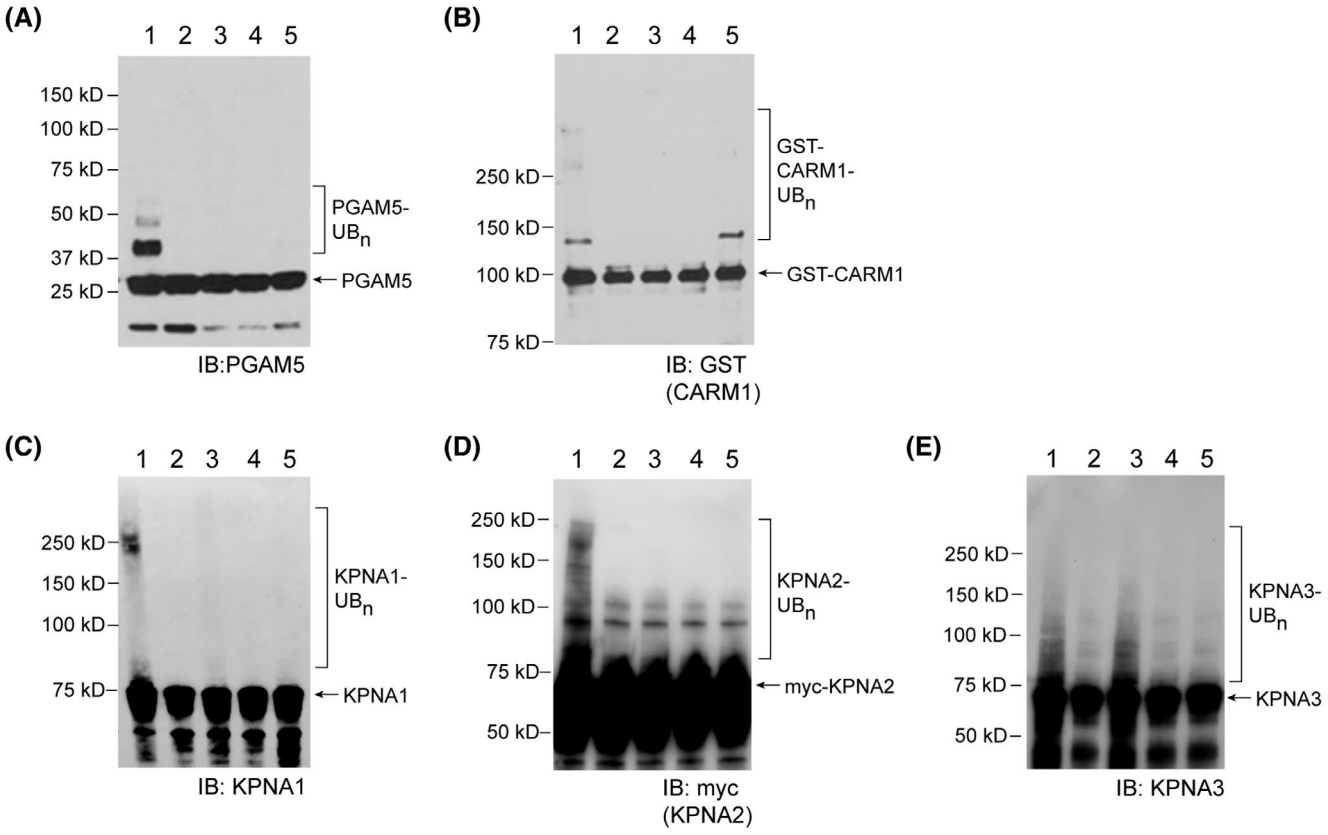

FIGURE 2 In vitro assays to verify protein ubiquitination catalyzed by the E6-E6AP pair. Reactivity of the E6-E6AP pair was assayed with substrates identified by orthogonal UB transfer, including (A) PGMA5, (B) CARM1, (C) KPNA1, (D) KPNA2, and (E) KPNA3. Ubiquitination reactions were set up with substrate proteins reacting with wt UB, Uba1, UBcH7, E6AP and E6 (reaction 1). The control reactions have all reaction components except for Uba1 (reaction 2), or UbcH7 (reaction 3), or E6AP (reaction 4), or E6 (reaction 5). SDS-PAGE gels of the reaction mixtures were blotted for Western analysis with antibodies against the substrates or the tags fused to the substrates

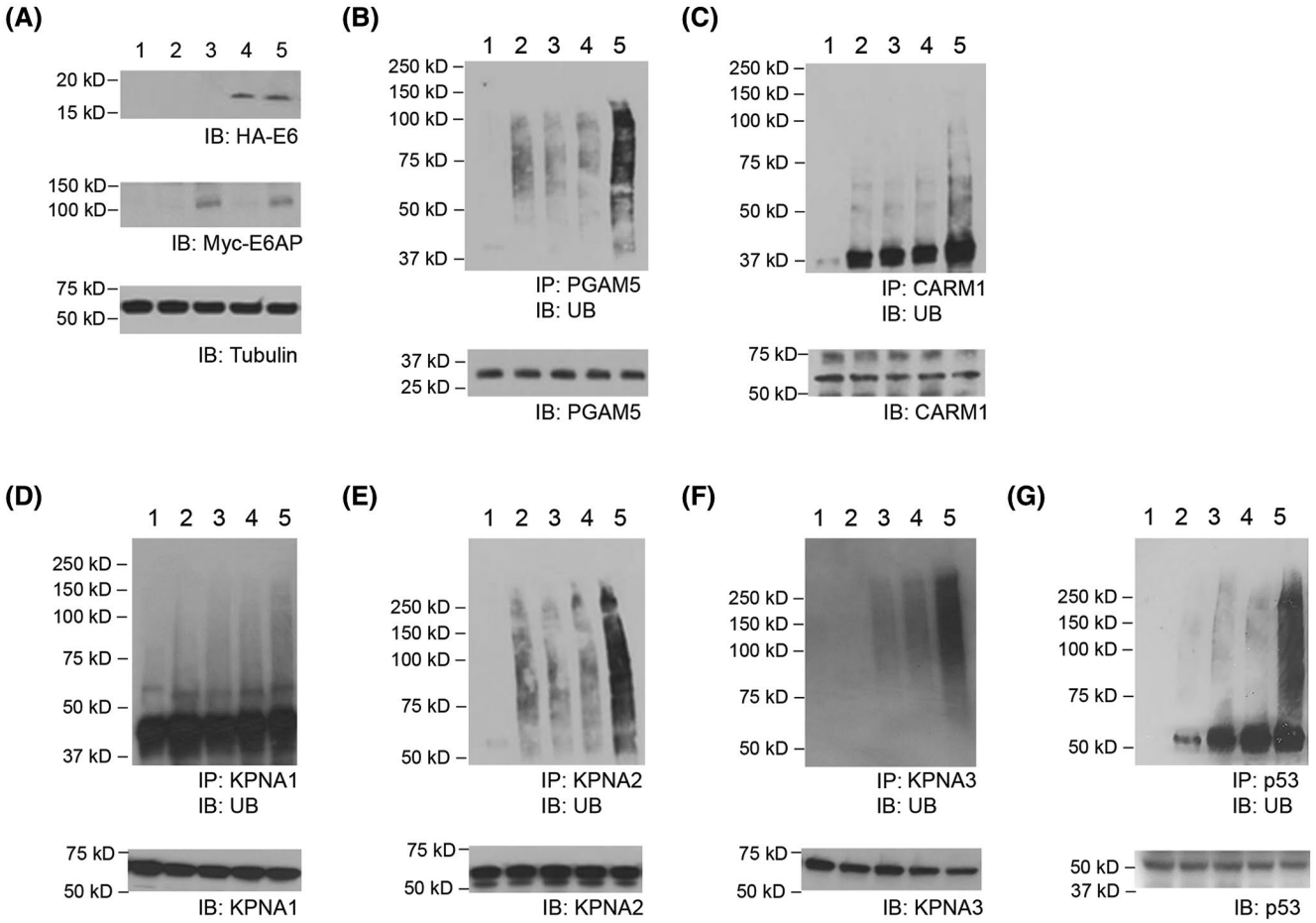

FIGURE 3 Verifying protein ubiquitination by the E6-E6AP pair in HEK293 cells. (A) Overexpression of E6 and E6AP were confirmed by probing with antibodies against the HA and myc tags fused to E6 and E6AP, respectively. (1) IgG control without incubating the cell lysate with the primary antibodies; (2) HEK293 cells; (3) cells transfected with pLenti-E6AP plasmid; (4) cells transfected with pLenti-E6 plasmid with the V42L mutation; (5) cells transfected with both pLenti-E6AP and pLenti-E6 plasmids. Ubiquitination of the substrate proteins identified by the orthogonal UB transfer screen was confirmed with (B) PGAM5, (C) CARM1, (D) KPNA1, (E) KPNA2, and (F) KPNA3 by immunoprecipitating the substrate proteins from cell lysate and measuring the level of ubiquitination with an anti-UB antibody. Assay of p53 ubiquitination was shown in (G) as a positive control. Lane assignment in (B)–(G) is the same as in (A), and the levels of the substrate proteins in the cell lysate were verified by immunoblotting with various anti-substrate antibodies (bottoms panels). Cells were treated with proteosome inhibitor MG132 to inhibit protein degradation 4 h before the cells were harvested to measure the ubiquitination levels of the substrate proteins

harvest, which was necessary for efficiently detecting polyubiquitinated forms of the substrate proteins. The expression of the E6AP and E6 in transfected HEK293 cells was confirmed by Western blot analysis, with the blots probed with antibodies against the myc and HA tags fused to E6AP and E6, respectively (Figure 3A). Lysates were immunoprecipitated with substrate-specific antibodies, followed by Western blotting for detecting the level of ubiquitination with an anti-UB antibody. We found substrate ubiquitination was significantly enhanced with the co-expression of E6 and E6AP (Figure 3B–F), so was polyubiquitination of p53 measured as a positive control (Figure 3G). These results confirm that the substrates identified by the OUT cascade of E6AP in the presence of E6 are bona fide ubiquitination targets of the E6-E6AP pair.

3.3 | The degradation of the substrate proteins was enhanced in E6AP-transfected HeLa cells

We then varied the level of exogenous E6AP expression in HPV-18-positive human cervical carcinoma HeLa cells that stably express E6[57] and determined the effects of E6AP expression on the steady-state levels of the substrates in the cells. At 24 h post-transfection with increasing amounts of the E6AP expression plasmid, cellular levels of the substrates were measured by Western blot analysis. We found increased expression of E6AP led to decreased steady-state levels of PGAM5, CARM1, and KPNA1-3, as well as p53, suggesting that E6AP would induce the degradation of the substrates in the HeLa cells with stable expression of E6

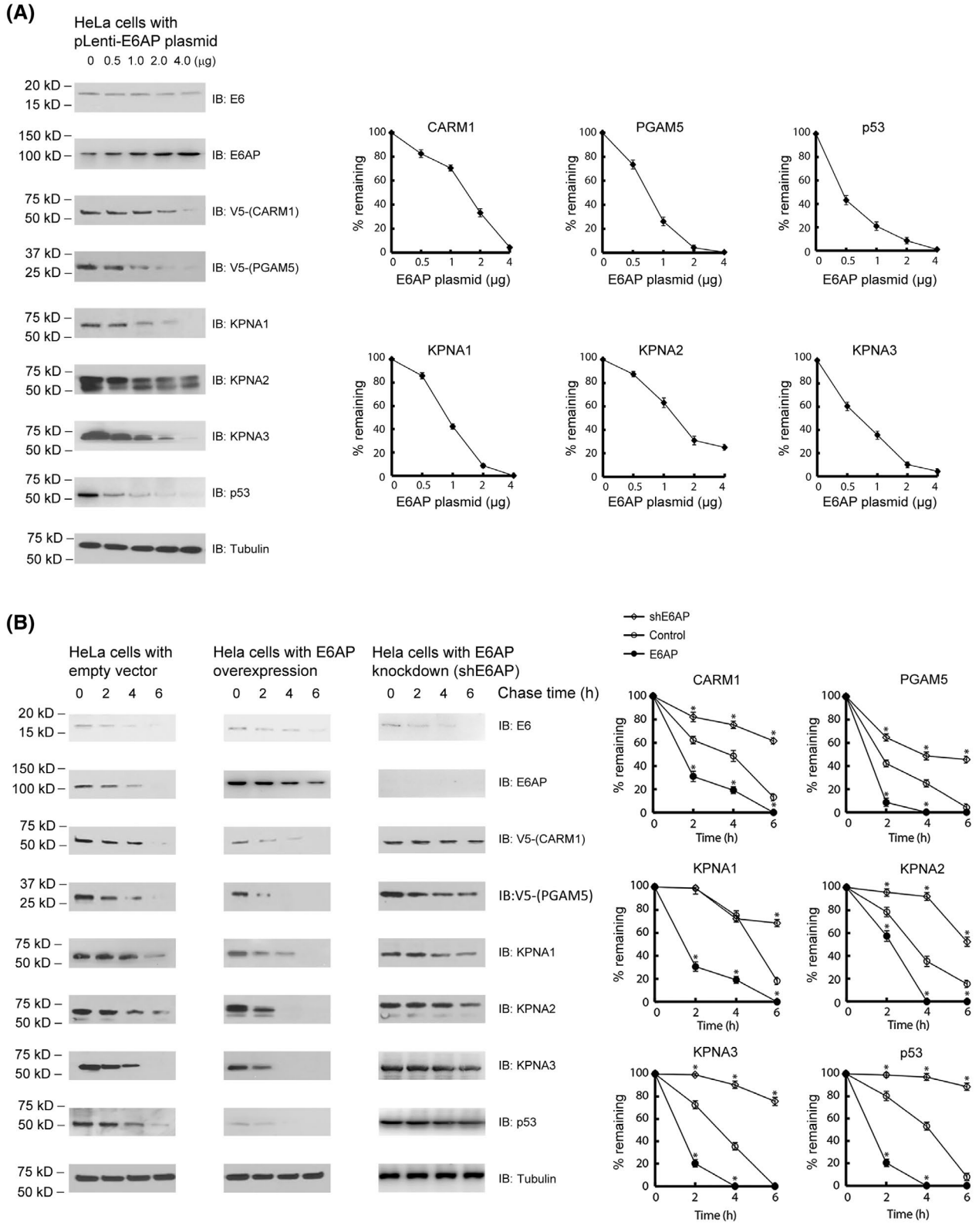

(Figure 4A). We also compared the degradation kinetics of the substrates in HeLa cells with and without elevated expression of E6AP. Cells transfected with or without the E6AP expression plasmid were treated with cycloheximide (CHX) to inhibit new protein synthesis. The substrate levels were measured at 2, 4, and 6 h of CHX treatment by Western blotting. The CHX chase experiment measured the stability of each substrate protein and demonstrated that the levels of the substrates decayed significantly faster in the E6AP overexpressing cells than in the control cells. In contrast, the substrate proteins gained prolonged stability in shE6AP cells with silenced E6AP expression (Figure 4B).

FIGURE 4 Substrate destabilization induced by the expression of E6AP in the HeLa cells. (A) Decreases in the steady-state levels of the substrate proteins caused by enhanced E6AP expression in the cell. HeLa cells were transfected with increasing amounts of the pLenti-E6AP plasmid, and the levels of the substrates were detected by Western blot analysis with antibodies binding to the substrate proteins or to the tags fused to the substrates. The steady state levels of p53 were assayed as a positive control. Changes of the steady state levels of the substrates with the amount of the pLenti-E6AP plasmid used for transfection were plotted in the panels on the right. (B) Destabilization of the substrate proteins in HeLa cells with E6AP expression as shown by the cycloheximide (CHX) chase assay. Cells were treated with CHX to inhibit protein synthesis and 2, 4, 6 h after the CHX addition, the cells were lysed, and the levels of the substrate proteins were measured by Western blot analysis. Changes of the substrate levels at various time points of CHX chase were measured in HeLa cells (left panels), HeLa cells with transfection of the E6AP expression plasmid (middle panels), and HeLa cells with the silenced expression of E6AP (right panels). Substrates in HeLa cells with enhanced E6AP expression showed faster protein degradation, in comparison with blank HeLa cells and cells with silenced expression of E6AP. Levels of p53 levels were also measured as a positive control. Quantitative analyses of the levels of the substrate proteins measured in the CHX chase assay were plotted in the panels on the right. The vertical bars in A and B represent SEM from three independent experiments ($n = 3$). *$p < .01$ versus control group

Consistently, similar accelerated degradation of p53 was observed in HeLa cells overexpressing E6AP. These results suggest the roles of E6AP and E6 in regulating the stabilities of the substrate proteins identified by OUT.

3.4 | The degradation of the substrate proteins was accelerated in HPV-negative C33A cells after E6 transfection

To further delineate the role of the E6-E6AP complex in controlling the stability of the newly identified substrates, we examined the steady-state levels and degradation kinetics of PGAM5, CARM1 and KPNA1-3 in HPV-negative human cervical cancer C33A cells with and without E6 transfection. C33A cells carry R273C mutation of p53, which is thought to be an oncogenic driver in the absence of E6 expression,[58,59] and this cell line has been widely used for studying the effects of forced E6 expression. Like E6AP expression in HeLa cells (Figure 4A), increasing expression of E6 resulted in the reduction of the steady-state levels of CARM1, PGAM5 and KPNA1 in C33A cells in dosage-dependent manners (Figure 5A). The levels of KPNA2 and KPNA3 also exhibited similar tendencies only to lesser extents. The stability of all these substrate proteins measured by the CHX chase experiment was significantly decreased in the E6-transfected C33A cells, compared with parental cells (Figure 5B). These experiments have provided further evidence that E6 expression promotes E6AP-mediated ubiquitination of these substrate proteins, leading to accelerated degradation.

3.5 | Inhibition of IFN-γ-induced nuclear import of STAT1 is mediated by E6-induced KPNA1 degradation

It is well established that IFN-γ induces phosphorylation of STAT1 through the activation of JAK1 and TYK2 kinases and KPNA1 recognizes phosphorylated STAT1-STAT2 dimer as cargos for transporting into the nucleus.[60,61] The nuclear translocation of the STAT dimers results in the activation of IFN-stimulated genes and the onset of the apoptotic program in virus-induced cancer cells including HeLa and ME-180.[62,63] We thus postulated that KPNA1 degradation induced by the E6-E6AP complex would limit the capacity of IFN signaling by restricting the rate of STAT1 nuclear translocation and diminish the antiviral response of host cells. To evaluate the hypothesis, we transfected varying amounts of the E6 vector into the HEK293 cells and treated the cells with IFN- γ for 30 min to activate the phosphorylation of STAT1 by JAK1 and TYK2. We then assayed the levels of KPNA1 in the cell and confirmed the negative correlation between E6 and KPNA1 level in the cell as we previously observed in C33A cells (Figures 6A and 5A). We also prepared cytoplasmic and nuclear extracts of the cells and probed the Western blot of the extracts with anti-STAT1 and anti-pSTAT1 antibodies. We found an increasing level of pSTAT1 in the cytoplasm and correspondingly a diminishing level of pSTAT1 in the nucleus with increasing expression of E6 in the cells (Figure 6B, left panels). The level of total STAT1 in the cytoplasm remained unaltered with increasing amounts of E6 expression, suggesting E6 did not affect the stability of STAT1 but rather altered the subcellular distribution of STAT1 between the cytoplasm and nucleus. In contrast, transfection with the same increasing amounts of the empty expression vector did not affect the ratio of nuclear and cytoplasmic pSTAT1 signals, indicating that the observed changes in nuclear and cytoplasmic levels of pSTAT1 were specific to E6 (Figure 6B, middle and right panels). These results suggest E6-triggered destabilization of KPNA1 plays a substantial role in preventing pSTAT1 from nuclear translocation and consequently causing cytoplasmic retention of pSTAT1.

To verify the E6-triggered changes in the subcellular distribution of pSTAT1, we examined the KPNA1 and STAT1 localization in HEK293 cells by immunofluorescence

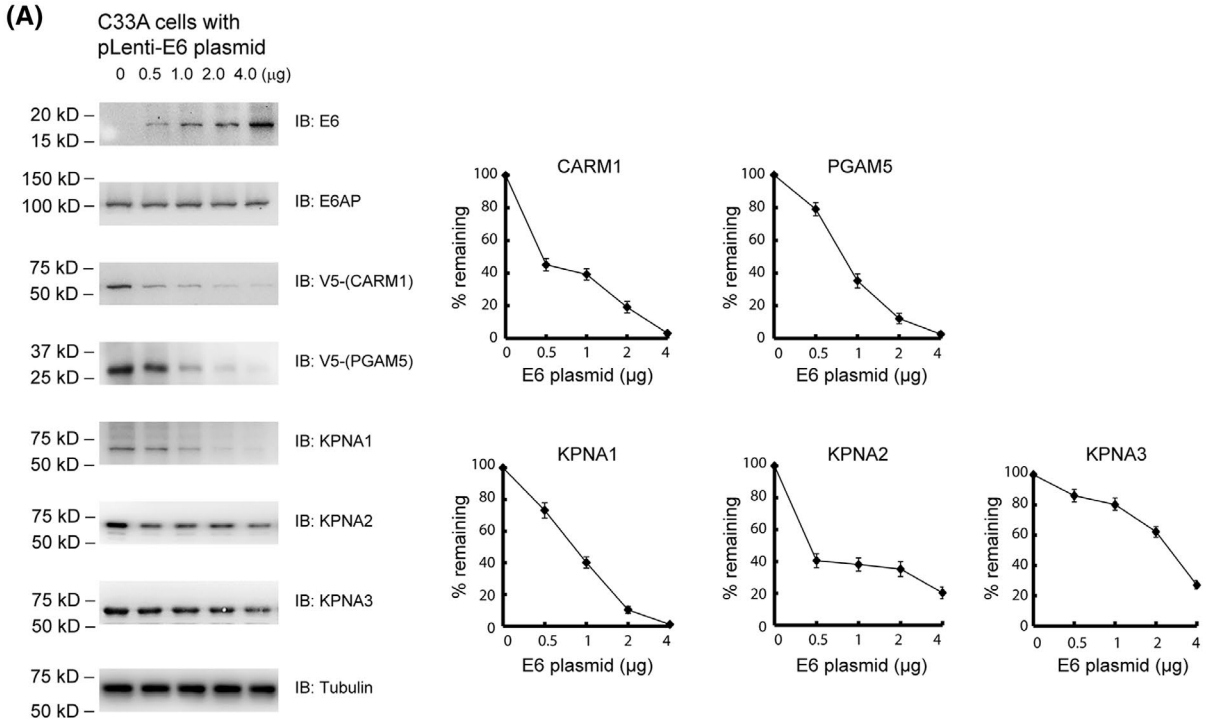

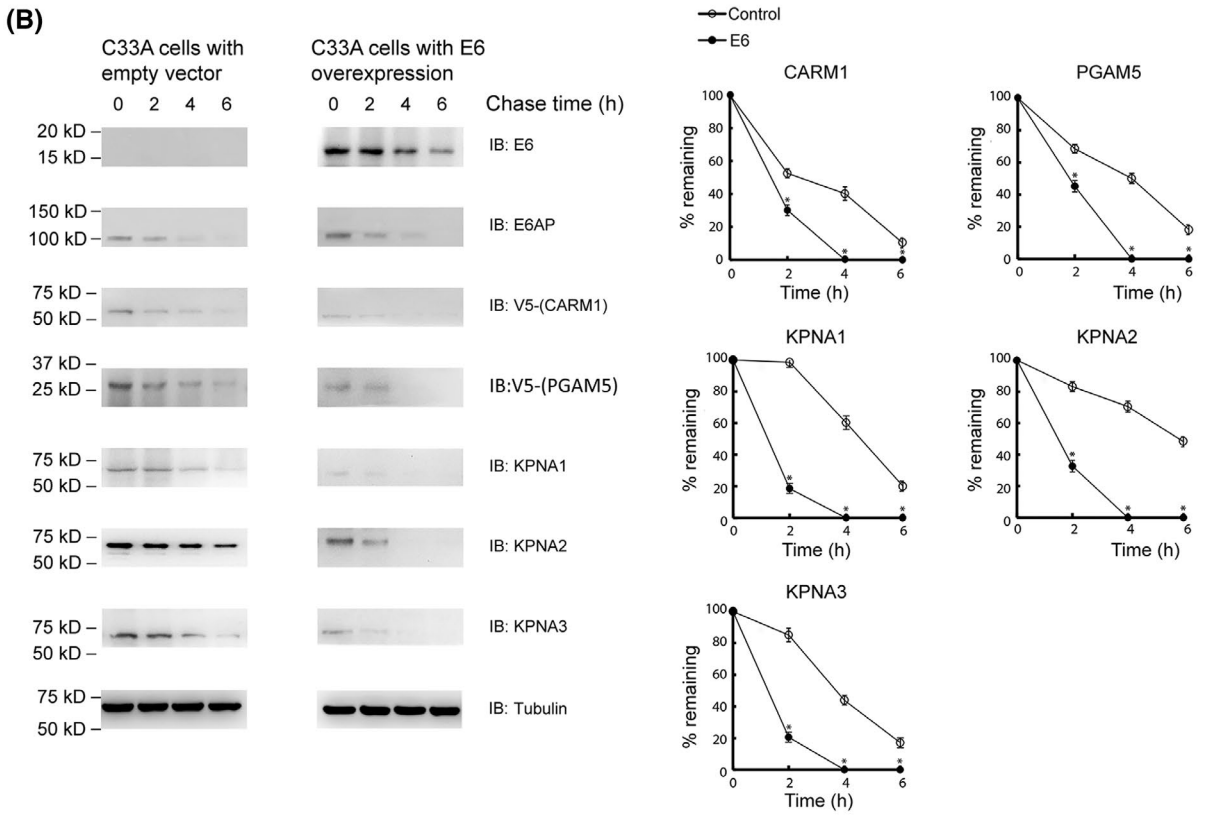

microscopy (Figure 6C). We transfected HEK293 cells with the vectors of E6 or E6AP, and stimulated the cells with IFN-γ for 30 min. We then stained the cells to visualize KPNA1 and pSTAT1. We found that without E6 expression, a significant fraction of pSTAT1 immunoreactivity, as well as KPNA1 immunoreactivity, was localized to the nucleus after IFN-γ stimulation of the cells (Figure 6C, upper panels). However, the distribution of pSTAT1 shifted from the nucleus to cytoplasm in the cells with E6 expression, which correlated with diminished levels of KPNA1 (Figure 6C, middle panels). These observations suggest that transfected E6 paired with endogenous E6AP

FIGURE 5 Substrate destabilization in C33A cells, an HPV-negative cervical cancer cell line with forced expression of E6. (A) Decreases in the steady-state levels of the substrate proteins caused by enhanced E6 expression in C33A cells. Cells were transfected with increasing amounts of the pLenti-E6 plasmid, and the levels of the substrates were detected by Western blot analysis with antibodies binding to the substrate proteins or to the tags fused to the substrates. Quantitative analysis of the change of the steady state levels of the substrates with the amount of the pLenti-E6 plasmid used for transfection was shown in the plots on the right. (B) Destabilization of the substrate proteins in C33A cells with E6 expression as shown by the cycloheximide (CHX) chase assay. Cells were treated with CHX to inhibit protein synthesis and 2, 4, 6 h after the CHX addition, the cells were lysed, and the levels of the substrate proteins were measured by Western blot analysis. Changes of the substrate levels at various time points of CHX chase were measured in C33A cells (left panels) and cells with transfection of the E6 expression plasmid (right panels). E6AP substrates showed faster degradation in C33A cells with overexpression of E6 compared to native cells. Levels of p53 were also assayed as a positive control. Quantitative analyses of the levels of the substrate proteins measured in the CHX chase assay were plotted in the panels on the right. The vertical bars in A and B represent SEM from three independent experiments ($n = 3$). *$p < .01$ versus control group

in the cells to destabilize KPNA1 and block nuclear translocation of pSTAT1. In contrast, E6AP overexpression alone did not result in decreased expression of KPNA1 or cytoplasmic retention of pSTAT1, indicating that E6 is required for the downregulation of KPNA1 and the inhibition of the nuclear translocation of pSTAT1 (Figure 6C, bottom panels).

3.6 | E6 protein inhibited IFN-γ-induced apoptosis of C33A cells

We next examined whether forced expression of E6 would affect IFN-γ-induced changes in the apoptotic program of C33A cells.[58] We transfected C33A cells with the E6 vector, and treated the cells with IFN-γ to activate the JAK-STAT pathway. We then used the TUNEL staining to identify apoptotic cells (Figure 7A). More than 20% of control cells without E6 expression were TUNEL positive after IFN-γ stimulation, indicating the legitimate activation of the JAK-STAT pathway leading to apoptosis. In contrast, only 2% of cells with E6 expression exhibited positive TUNEL staining, suggesting that E6 suppressed the proapoptotic pathway downstream of the IFN-γ signaling pathway. Cells transfected with the blank vector underwent apoptosis to a similar extent as the cells with no transfection, indicating that the inhibition of apoptotic response to IFN-γ was dependent on the forced expression of E6. We further analyzed molecular characteristics of IFN-γ-induced apoptotic response, such as the cleavage of caspases and upregulation of the pro-apoptotic proteins Bim, FAS, and nitric oxide synthase (iNOS), in C33A cells with or without exogenous E6 expression. We observed that the cells with forced E6 expression displayed decreased levels of the cleaved forms of caspases 3/8/9 at 30 min after IFN-γ stimulation, in comparison with the cells without E6 expression or those with E6AP overexpression (Figure 7B). There were similar levels of un-cleaved caspases in IFN-γ-treated cells with and without E6 expression. The expression levels of Bim, FAS and iNOS were all upregulated in IFN-γ-treated cells without E6 expression, as expected. C33A cells with forced E6 expression showed significant suppression of the IFN-γ-dependent upregulation of those proapoptotic genes (Figure 7C). These results suggest that the presence of E6 can suppress the antiviral pro-apoptotic program, at least partly by destabilizing KPNA1 and blocking the nuclear translocation of pSTAT1 (Figure 8). We performed similar assays with HeLa cells, and again, the results showed that enhanced expression of E6 inhibited the cleavage of caspase 3/8/9 and lowered the expression of Bim in cells with IFN-γ stimulation (Figure S1).

4 | DISCUSSION

In this study, we used the OUT method to follow xUB transfer from E6AP to its ubiquitination targets in the presence of E6 and identified a substrate pool of E6AP facilitated by the E6-E6AP interaction. Previously, affinity-based screens, including yeast two-hybrid (Y2H) systems, split luciferase assays, and affinity purification of E6-bound protein complexes, have been developed to profile E6-interaction networks to decipher the roles of the viral oncoprotein on various cellular processes.[64] Y2H with E6 as the bait identified 94 interacting proteins, including four interactors previously reported (TADA3L, SIPA1L1, 1RF3a, and Smad3).[65] The screen with the split luciferase in HEK293 cells identified 97 potential protein interactors of E6. Among them, about one-third of the interactors, including E6AP, Smad3, Smad4, BRCA1, and IRF7, were found to have strong interactions with E6.[65] The split luciferase assay was also used to screen for E6 interactors within a pool of 590 proteins of the ubiquitin-proteasome system consisting of UB transfer enzymes E1, E2, and E3, deubiquitinating enzymes (DUB), and proteasome subunits.[51] Besides reconfirming the binding of E6 with HECT E6AP, the screen identified new interactions between E6 and Ring E3s MGRN1, LNX3, and LNX4, and suggested the potential role of E6 in stirring the substrate

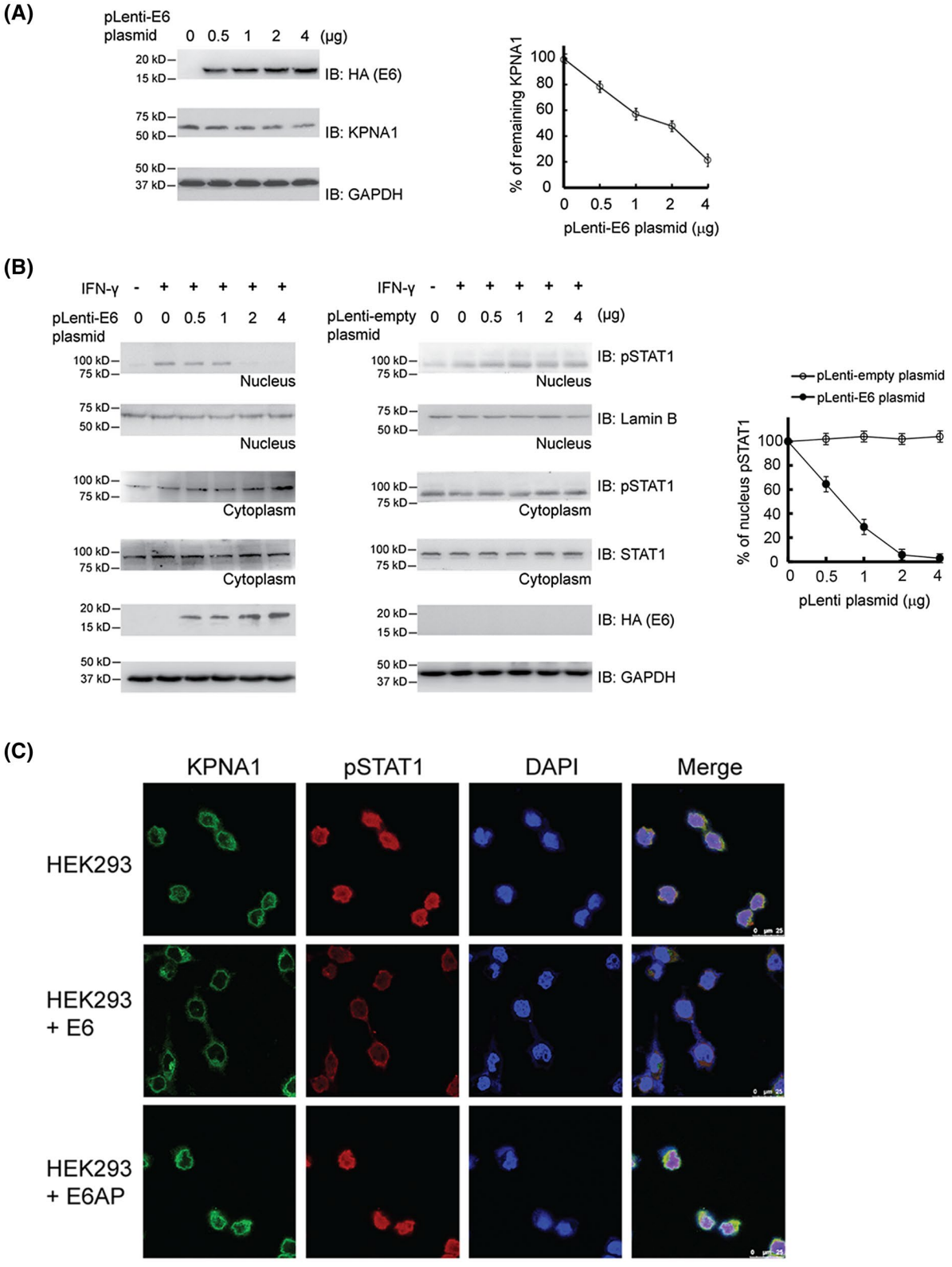

specificities of multiple E3s. MS-based proteomics has the advantage of identifying E6 complexes in the physiological context of the cell. Using an affinity-tagged E6 to co-immunoprecipitate host cell proteins, numerous E6 partners were identified including HECT E3s E6AP and HERC2, components of the Ring E3 Ccr4-Not complex, acetyltransferase CBP and p300, transcription factors MAML1, CEBPB, and NFKB1, and a number of proteasome subunits.[50,52] Recently a UB mutant with the K48R and K63R mutations was found to be preferentially used by the E6-E6AP pair to ubiquitinate substrate proteins comparing to E6AP along. So the biotin-conjugated UB

FIGURE 6 E6-mediated destabilization of KPNA1 reduced the translocation of phosphorylated STAT1 (pSTAT1) into the nucleus. (A) Increased expression of HA-E6 resulted in the decreasing level of KPNA1 in the HEK293 cells. Increasing amounts of the expressing vector of HA-E6 were used for transient transfection of HEK293 cells, and the Western blots of the cell lysates were probed with antibodies against HA-E6 and KPNA1 to detect their expression levels. The panel on the right plots the change in KPNA1 expression levels against the increasing amounts of E6 expression plasmid used for transfection. (B) Increased E6 expression in HEK293 cells leads to less transport of pSTAT1 into nucleus and more accumulation of pSTAT1 in the cytoplasm. Increasing amounts of pLenti-E6 vector were used for transient transfection of HEK293 cells. The cells were stimulated by IFN-γ followed by Western blot analysis of the levels of STAT1 and pSTAT1 in the nuclear and cytoplasmic extracts of the cells (left panels). As a control, same amounts of empty pLenti vectors were used to transfect HEK293 cells and after IFN-γ stimulation, the nuclear and cytoplasmic extracts were analyzed by Western blotting probed with anti-STAT1 and anti-pSTAT1 antibodies (middle panels). The panel on the right plots the changes of nuclear pSTAT1 levels with increasing amounts of E6 expression plasmid used for transfection. In (A) and (B), blots from three independent experiments were used for calculation of the mean ± S.E. (C) Immunofluorescence imaging of pSTAT1 transportation into the nucleus in HEK293 cell without E6 expression (upper row), with E6 expression (middle row) and with only enhanced expression of E6AP (bottom row). Cells were stained with antibodies against KPNA1 and pSTAT1 to reveal the levels and localization of the two proteins (left two columns), and stained with DAPI to reveal the boundary of the nucleus (second column from the right). Images showing the staining by anti-KPNA1 antibody and DAPI were merged (column on the right). The panels show data representative of experiments with at least three biological replicates. Data points show mean ± S.E. of three or more experiments. The vertical bars in A and B represent SEM from three independent experiments ($n = 3$)

mutant was added to cell lysates with externally supplied E6 and the enzymes of the E6AP cascade. Proteins with biotin-UB conjugation were affinity-purified and identified by proteomics. Among them, XRCC4, a protein of the DNA repair pathway, and OTUD5, a DUB, were confirmed as the substrates of the E6-6AP pair.[66] This approach based on in vitro reactions has provided useful information about E6-E6AP-meiated ubiquitination, which would be complementary with our OUT-based screening in cells.

OUT differs from the affinity-based screens with E6 in that it identifies the changes in the substrate profile of E6AP upon the association of E6 with E6AP; so it can reveal the direct impact of E6 expression on the cellular context by stirring the ubiquitination targets of E6AP. Therefore, OUT is a focused and catalysis-based approach based on the UB transfer reaction to delineate the roles of E6 in governing HPV infection. Since HBT-xUB, E6, and all the OUT components of E6AP are expressed in the cell, the substrates of E6-E6AP are conjugated with HBT-xUB in their native states. E6 not only functions as an adaptor to recruit substrates such as transcription factors p53 and NFX1-91 to E6AP, but also acts as an allosteric activator of E6AP to enhance its ubiquitination of its original substrate pool.[67] The OUT screen, by tracking UB transfer from E6AP to its cellular substrates in the presence and absence of E6, can identify both new substrates of E6AP bridged by the E6 adaptor and the original substrates of E6AP with enhanced ubiquitination due to allosteric activation of E6AP by E6 (Tables S1 and S2). The in vitro ubiquitination assays indeed suggest that E6AP can weakly ubiquitinate CARM1 and KPNA1 in the absence of E6, but the association of E6 with E6AP enhanced its activity in ubiquitinating these two substrates (Figures 2 and 3). It would be of interest to carry out further analysis to differentiate the roles of E6 as an adaptor or an allosteric activator in mediating UB transfer from E6AP to its substrate pool identified by the OUT screen.

In the present study, we used HEK293 cells as a platform for the OUT screen, whereas this cell line is not directly relevant to HPV-induced oncogenesis. HEK293 cells are one of the most widely used cell lines for proteomic analyses and have become a standard in the interactome databases, providing abundant and reliable datasets on differential protein expression profiles and protein-protein interactions. This cell line also exhibits excellent efficiency of plasmid transfection and viral transduction, which enables the optimal expression of the OUT components, that is, xE1, xE2, xE3, and HBT-xUB. Our previous OUT screens for substrates of E6AP (without E6), E4B, and CHIP successfully used HEK293 cells,[32,34] which allowed us to perform quality control by comparative analysis among the datasets. Nonetheless, using more disease-relevant cell types, for example, non-transformed keratinocytes, would be ideal for determining E6-E6AP targets by OUT screens. Our ongoing investigation to develop OUT systems in clinically relevant cell types, such as pluripotent stem cells, is expected to provide novel cell models in which physiological substrates of disease-associated E3s can be profiled efficiently.

OUT profiling the substrates of the E6-E6AP pair revealed a role of E6 in stimulating KPNA1 ubiquitination by E6AP to subvert the IFN signaling pathway, a key antiviral defense system of the host cell. OUT identified KPNA1-3 of the importin α family as E6AP substrates in the presence of E6 (Figure 8). In particular, our data suggest that E6-induced ubiquitination of KPNA1 plays a key role in hampering IFN signaling and protecting host cells from apoptotic response to HPV infection (Figure 6). In the presence of E6 expression, KPNA1 actively undergoes proteasomal degradation, and such persistent

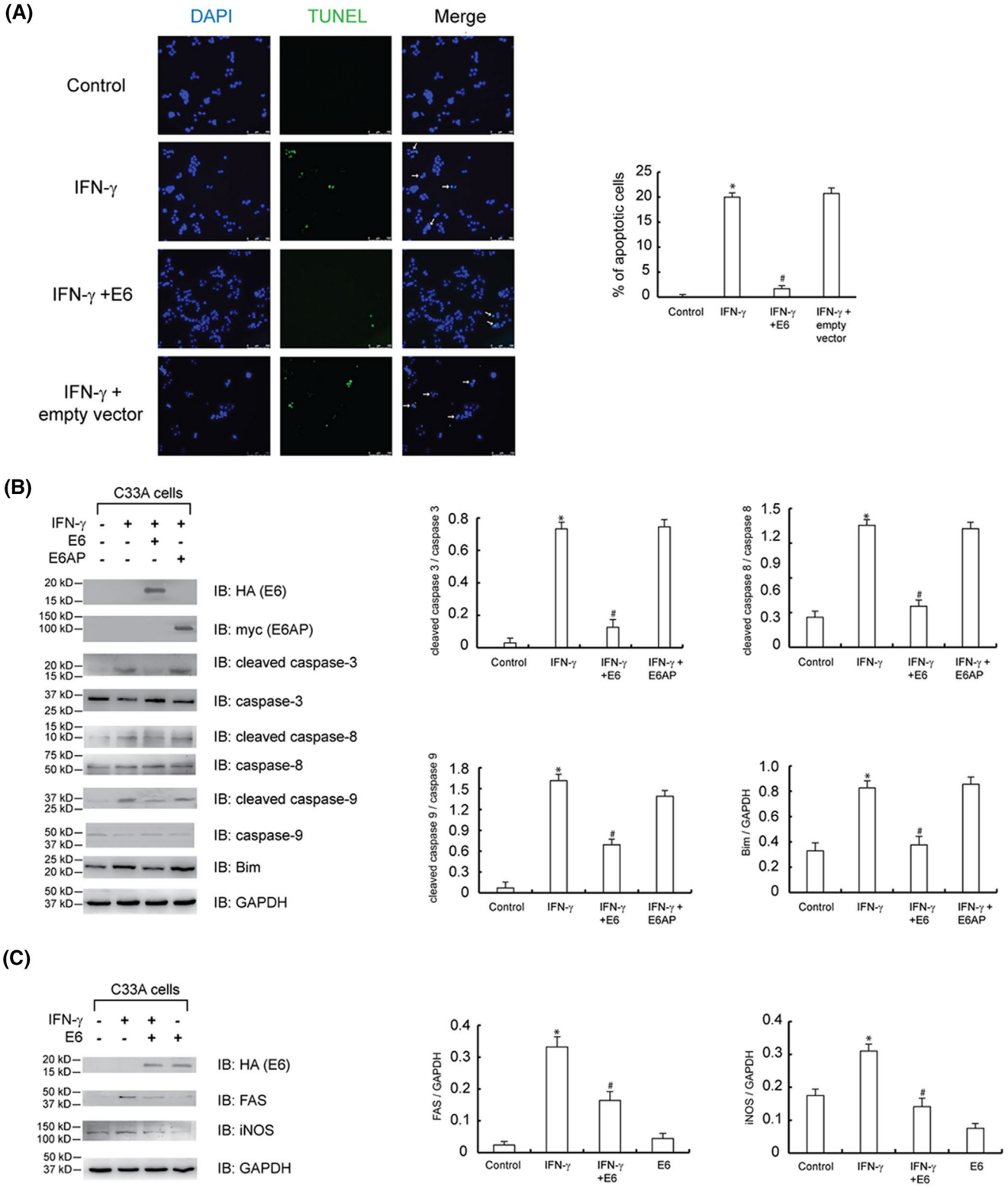

downregulation of the importin-α complex results in suppression of the nuclear translocation of phosphorylated STAT1, the rate-limiting step of the proapoptotic IFN signaling (Figure 6). As a consequence, cells expressing E6 become more refractory to IFN-mediated anti-apoptotic response, as demonstrated by our analysis on caspase cleavage and the IFN-responsive genes such as Bim, FAS, and iNOS (Figure 7). Previously E6 has been found to bind to TYK2 kinase of the JAK-STAT pathway and inhibit its activation by IFN-α and it can also bind to IRF3, a downstream target of the Toll-like receptor pathway, to block its transcriptional activity for IFN synthesis.[68,69] Our

FIGURE 7 Counteraction of E6 on apoptosis in C33A cells stimulated by IFN-γ. (A) Comparison of the TUNEL images of apoptotic cells with and without E6 expression in C33A cells after stimulating the cells with IFN-γ. Representative images from at least three independent experiments were shown. The numbers of apoptotic cells were counted based on the TUNEL images and plotted in the panel on the right to show 10-fold less apoptotic cells with E6 expression than the cells without E6 expression. The apoptotic cells were counted in five randomly selected fields for each sample to calculate the mean ± S.E. (B) Decreased levels of apoptotic markers in the cells expressing E6 comparing to cells without E6 expression after IFN-γ stimulation. E6 expression in cells stimulated by IFN-γ significantly suppressed the cleavage of caspases 3/8/9 and the level of proapoptotic protein Bim. The level of cleaved caspases and the expression of Bim with and without E6 expression were plotted in the panels on the right. (C) E6 expression suppressed the cellular levels of FAS and iNOS after IFN-γ stimulation. The expression levels of FAS and iNOS in cells after various treatments were plotted in the panels on the right. In (B) and (C), blots from three independent experiments were used for quantification purposes and representative blots are shown. Data points show mean ± S.E. of three or more experiments. The vertical bars in A, B and C represent SEM from three independent experiments ($n = 3$). $^{*}p < .01$ versus control group. $^{\#}p < .01$ versus IFN-γ group

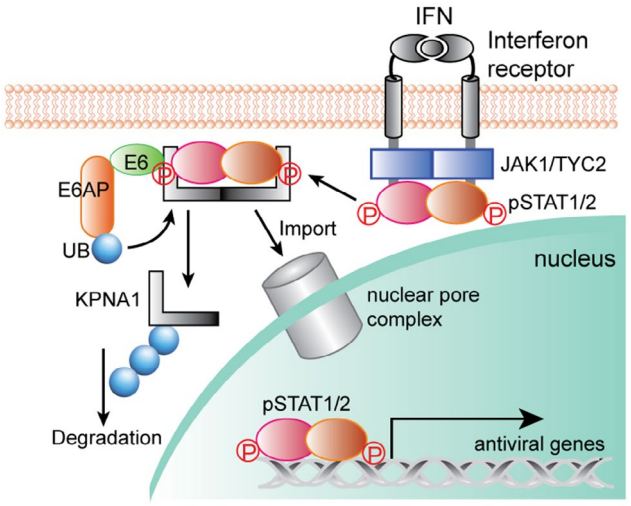

FIGURE 8 Inhibition of the JAK-STAT pathway through E6-mediated ubiquitination of KPNA1 by E6AP. Activation of the interferon (IFN) receptors would lead to the phosphorylation of transcription factors STAT1 and STAT2 by the JAK1 and TYK2 kinases. Phosphorylated STAT1 and STAT2 (pSTAT1/2) are recognized as the cargo proteins by importin α proteins such as KPNA1 for transportation into the nucleus. Once in the nucleus, pSTAT1/2 would active the expression of antiviral genes including the genes that would induce apoptosis of the cells infected by the virus. In this study, we found E6 protein of HPV16 could mediate UB transfer from E6AP to KPNA1 to induce its degradation by the proteasome. E6 expression in the host cell would inhibit translocation of pSTAT1 into nucleus after stimulation of the cell by IFN-γ and thus block activation of proapoptotic genes

work has thus established a new mechanism of HPV E6 in downregulating the IFN-γ-induced apoptosis of cervical cancer cells by affecting the nuclear transport of the key signaling proteins that activate IFN-responsive genes (Figure 8).

The nuclear envelop is a physical barrier separating the signaling proteins of the host or viral origin in the cytoplasm and the genetic codes for cell regulation in the nucleus. It is not surprising that viruses have evolved diverse strategies to manipulate the nuclear transport system to evade antiviral response of the host and to boost the chance of virus proliferation.[54,70] ORF6 of the SARS-CoV-1 can bind to KPNA2-KPNB1 complex and sequester it to the ER-Golgi membrane to deplete KPNB1 from forming a complex with KPNA1 for transporting phosphorylated STAT1 across the nuclear membrane.[71] VP24 of Ebolavirus binds directly to KPNA1 to interfere with STAT1 trafficking to the nucleus. Besides binding, virus has evolved strategies to trigger the proteolytic cleavage of KPNA1 to mask its activity. The 3Cpro protease of the foot-and-mouse disease virus can cleave KPNA1,[72] and the NSP1β protein of the porcine reproductive and respiratory syndrome virus (PRRSV) can enhance the ubiquitination of KPNA1 and destabilize it to inhibit its activity in IFN-dependent response to virus invasion.[73] NSP1β does not function as a E3 UB ligase by itself, and the host E3 pairing with NSP1β for KPNA1 ubiquitination is yet to be identified. It would be of interest to test if NSP1β would be associated with E6AP to ubiquitinate KPNA1 in the porcine host cells. Our work on E6/E6AP-dependent regulation of KPNA1 stability provides a novel perspective of virus coercing of protein ubiquitination pathways in the host cell to disarm apoptotic response and may be further explored for the development of counteracting therapeutics.

ACKNOWLEDGMENTS

This work was supported by grants from NIH (R01GM104498 to J.Y. and H.K.) and NSF (1710460 and 2109051 to J.Y.) of US, by the Simons Foundation Autism Research Initiative (to H.K.), and by Fundamental Research Funds for the Central Universities of China (21619329 to Y.W.). We are grateful to Dr. Peter M. Howley of Harvard Medical School for helpful discussions and Dr. Jon M. Huibregtse of the University of Texas at Austin for kindly sharing the expression plasmids of E6AP.

DISCLOSURES

The authors declare that they have no conflicts of interest with the content of this article.

AUTHOR CONTRIBUTIONS

Y.W., H.W., H.K., and J.Y. conceived the idea and designed the experiments. Y.W., R.L., J.L., L.J., G.H.J., L.Z., M.P., D.D. performed experiments. N.T.S. provided technical guidance. Y.W., R.L., D.D., H.W., H.K., and J.Y. analyzed data, interpreted results, drafted and edited the manuscript. Y.W., H.W., H.K., and J.Y. acquired funding. All authors reviewed and approved the final version of the manuscript.

ORCID

Yiyang Wang https://orcid.org/0000-0002-0318-6715
Jun Yin https://orcid.org/0000-0002-4803-7510

REFERENCES

1. Cogliano V, Baan R, Straif K, et al. Carcinogenicity of human papillomaviruses. *Lancet Oncol*. 2005;6:204.
2. zur Hausen H. Papillomaviruses in human cancers. *Proc Assoc Am Phys*. 1999;111:581-587.
3. Thomas M, Narayan N, Pim D, et al. Human papillomaviruses, cervical cancer and cell polarity. *Oncogene*. 2008;27:7018-7030.
4. de Villiers E-M, Fauquet C, Broker TR, et al. Classification of papillomaviruses. *Virology*. 2004;324:17-27.
5. Steben M, Duarte-Franco E. Human papillomavirus infection: epidemiology and pathophysiology. *Gynecol Oncol*. 2007;107:S2-S5.
6. Snijders PJ, Steenbergen RD, Heideman DA, Meijer CJ. HPV-mediated cervical carcinogenesis: concepts and clinical implications. *J Pathol*. 2006;208:152-164.
7. Tomaic V. Functional roles of E6 and E7 oncoproteins in HPV-induced malignancies at diverse anatomical sites. *Cancers (Basel)*. 2016;8:95.
8. Munger K, Phelps WC, Bubb V, Howley PM, Schlegel R. The E6 and E7 genes of the human papillomavirus type 16 together are necessary and sufficient for transformation of primary human keratinocytes. *J Virol*. 1989;63:4417-4421.
9. Huibregtse JM, Scheffner M, Howley PM. A cellular protein mediates association of p53 with the E6 oncoprotein of human papillomavirus types 16 or 18. *EMBO J*. 1991;10:4129-4135.
10. Scheffner M, Werness BA, Huibregtse JM, Levine AJ, Howley PM. The E6 oncoprotein encoded by human papillomavirus types 16 and 18 promotes the degradation of p53. *Cell*. 1990;63:1129-1136.
11. Scheffner M, Huibregtse JM, Vierstra RD, Howley PM. The HPV-16 E6 and E6-AP complex functions as a ubiquitin-protein ligase in the ubiquitination of p53. *Cell*. 1993;75:495-505.
12. Huh K-W, DeMasi J, Ogawa H, et al. Association of the human papillomavirus type 16 E7 oncoprotein with the 600-kDa retinoblastoma protein-associated factor, p600. *Proc Natl Acad Sci USA*. 2005;102:11492-11497.
13. Huh K, Zhou X, Hayakawa H, et al. Human papillomavirus type 16 E7 oncoprotein associates with the cullin 2 ubiquitin ligase complex, which contributes to degradation of the retinoblastoma tumor suppressor. *J Virol*. 2007;81:9737-9747.
14. Wallace NA, Galloway DA. Novel functions of the human papillomavirus E6 oncoproteins. *Annu Rev Virol*. 2015;2:403-423.
15. Đukić A, Lulić L, Thomas M, et al. HPV oncoproteins and the ubiquitin proteasome system: a signature of malignancy? *Pathogens*. 2020;9:133.
16. Vande Pol SB, Klingelhutz AJ. Papillomavirus E6 oncoproteins. *Virology*. 2013;445:115-137.
17. Underbrink MP, Howie HL, Bedard KM, Koop JI, Galloway DA. E6 proteins from multiple human betapapillomavirus types degrade Bak and protect keratinocytes from apoptosis after UVB irradiation. *J Virol*. 2008;82:10408-10417.
18. Thomas M, Banks L. Inhibition of Bak-induced apoptosis by HPV-18 E6. *Oncogene*. 1998;17:2943-2954.
19. Nakagawa S, Huibregtse JM. Human scribble (Vartul) is targeted for ubiquitin-mediated degradation by the high-risk papillomavirus E6 proteins and the E6AP ubiquitin-protein ligase. *Mol Cell Biol*. 2000;20:8244-8253.
20. Handa K, Yugawa T, Narisawa-Saito M, et al. E6AP-dependent degradation of DLG4/PSD95 by high-risk human papillomavirus type 18 E6 protein. *J Virol*. 2007;81:1379-1389.
21. Jing M, Bohl J, Brimer N, Kinter M, Vande Pol SB. Degradation of tyrosine phosphatase PTPN3 (PTPH1) by association with oncogenic human papillomavirus E6 proteins. *J Virol*. 2007;81:2231-2239.
22. Bedard KM, Underbrink MP, Howie HL, Galloway DA. The E6 oncoproteins from human betapapillomaviruses differentially activate telomerase through an E6AP-dependent mechanism and prolong the lifespan of primary keratinocytes. *J Virol*. 2008;82:3894-3902.
23. Xu M, Luo W, Elzi DJ, Grandori C, Galloway DA. NFX1 interacts with mSin3A/histone deacetylase to repress hTERT transcription in keratinocytes. *Mol Cell Biol*. 2008;28:4819-4828.
24. Gross-Mesilaty S, Reinstein E, Bercovich B, et al. Basal and human papillomavirus E6 oncoprotein-induced degradation of Myc proteins by the ubiquitin pathway. *Proc Natl Acad Sci USA*. 1998;95:8058-8063.
25. Jha S, Vande Pol S, Banerjee NS, et al. Destabilization of TIP60 by human papillomavirus E6 results in attenuation of TIP60-dependent transcriptional regulation and apoptotic pathway. *Mol Cell*. 2010;38:700-711.
26. Subbaiah VK, Zhang Y, Rajagopalan D, et al. E3 ligase EDD1/UBR5 is utilized by the HPV E6 oncogene to destabilize tumor suppressor TIP60. *Oncogene*. 2016;35:2062-2074.
27. Storrs CH, Silverstein SJ. PATJ, a tight junction-associated PDZ protein, is a novel degradation target of high-risk human papillomavirus E6 and the alternatively spliced isoform 18 E6. *J Virol*. 2007;81:4080-4090.
28. Vats A, Thatte J, Banks L. Identification of E6AP-independent degradation targets of HPV E6. *J Gen Virol*. 2019;100:1674-1679.
29. Massimi P, Shai A, Lambert P, Banks L. HPV E6 degradation of p53 and PDZ containing substrates in an E6AP null background. *Oncogene*. 2008;27:1800-1804.
30. Hsu C-H, Peng K-L, Jhang H-C, et al. The HPV E6 oncoprotein targets histone methyltransferases for modulating specific gene transcription. *Oncogene*. 2012;31:2335-2349.
31. Tan MJ, White EA, Sowa ME, et al. Cutaneous beta-human papillomavirus E6 proteins bind Mastermind-like coactivators and repress Notch signaling. *Proc Natl Acad Sci USA*. 2012;109:E1473-E1480.
32. Wang Y, Liu X, Zhou LI, et al. Identifying the ubiquitination targets of E6AP by orthogonal ubiquitin transfer. *Nat Commun*. 2017;8:2232.
33. Zhao B, Bhuripanyo K, Zhang K, et al. Orthogonal ubiquitin transfer through engineered E1–E2 cascades for protein ubiquitination. *Chem Biol*. 2012;19:1265-1277.

34. Bhuripanyo K, Wang Y, Liu X, et al. Identifying the substrate proteins of U-box E3s E4B and CHIP by orthogonal ubiquitin transfer. *Sci Adv*. 2018;4:e1701393.
35. Wang Y, Fang S, Chen G, et al. Regulation of the endocytosis and prion-chaperoning machineries by yeast E3 ubiquitin ligase Rsp5 as revealed by orthogonal ubiquitin transfer. *Cell Chem Biol*. 2021;28:1283-1297.e8.
36. Miyamoto Y, Yamada K, Yoneda Y. Importin alpha: a key molecule in nuclear transport and non-transport functions. *J Biochem*. 2016;160:69-75.
37. Cagatay T, Chook YM. Karyopherins in cancer. *Curr Opin Cell Biol*. 2018;52:30-42.
38. Kau TR, Way JC, Silver PA. Nuclear transport and cancer: from mechanism to intervention. *Nat Rev Cancer*. 2004;4:106-117.
39. Tessier TM, Dodge MJ, Prusinkiewicz MA, Mymryk JS. Viral appropriation: laying claim to host nuclear transport machinery. *Cells*. 2019;8:559.
40. Nardozzi J, Wenta N, Yasuhara N, Vinkemeier U, Cingolani G. Molecular basis for the recognition of phosphorylated STAT1 by importin alpha5. *J Mol Biol*. 2010;402:83-100.
41. McBride KM, Banninger G, McDonald C, Reich NC. Regulated nuclear import of the STAT1 transcription factor by direct binding of importin-alpha. *EMBO J*. 2002;21:1754-1763.
42. Fagerlund R, Melen K, Kinnunen L, Julkunen I. Arginine/lysine-rich nuclear localization signals mediate interactions between dimeric STATs and importin alpha 5. *J Biol Chem*. 2002;277:30072-30078.
43. Yang F, Li S, Cheng Y, Li J, Han X. Karyopherin alpha 2 promotes proliferation, migration and invasion through activating NF-kappaB/p65 signaling pathways in melanoma cells. *Life Sci*. 2020;252:117611.
44. Liang P, Zhang H, Wang G, et al. KPNB1, XPO7 and IPO8 mediate the translocation of NF-kappaB/p65 into the nucleus. *Traffic*. 2013;14:1132-1143.
45. Welch K, Franke J, Kohler M, Macara IG. RanBP3 contains an unusual nuclear localization signal that is imported preferentially by importin-alpha3. *Mol Cell Biol*. 1999;19:8400-8411.
46. Marchenko ND, Hanel W, Li D, et al. Stress-mediated nuclear stabilization of p53 is regulated by ubiquitination and importin-alpha3 binding. *Cell Death Differ*. 2010;17:255-267.
47. Sailer C, Offensperger F, Julier A, et al. Structural dynamics of the E6AP/UBE3A-E6-p53 enzyme-substrate complex. *Nat Commun*. 2018;9:4441.
48. Zanier K, Charbonnier S, Sidi AOMO, et al. Structural basis for hijacking of cellular LxxLL motifs by papillomavirus E6 oncoproteins. *Science*. 2013;339:694-698.
49. Grace M, Munger K. Proteomic analysis of the gamma human papillomavirus type 197 E6 and E7 associated cellular proteins. *Virology*. 2017;500:71-81.
50. White EA, Kramer RE, Tan MJA, et al. Comprehensive analysis of host cellular interactions with human papillomavirus E6 proteins identifies new E6 binding partners and reflects viral diversity. *J Virol*. 2012;86:13174-13186.
51. Poirson J, Biquand E, Straub M-L, et al. Mapping the interactome of HPV E6 and E7 oncoproteins with the ubiquitin-proteasome system. *FEBS J*. 2017;284:3171-3201.
52. Rozenblatt-Rosen O, Deo RC, Padi M, et al. Interpreting cancer genomes using systematic host network perturbations by tumour virus proteins. *Nature*. 2012;487:491-495.
53. Kang YJ, Bang B-R, Han KH, et al. Regulation of NKT cell-mediated immune responses to tumours and liver inflammation by mitochondrial PGAM5-Drp1 signalling. *Nat Commun*. 2015;6:8371.
54. Cautain B, Hill R, de Pedro N, Link W. Components and regulation of nuclear transport processes. *FEBS J*. 2015;282:445-462.
55. Schneider-Gadicke A, Schwarz E. Different human cervical carcinoma cell lines show similar transcription patterns of human papillomavirus type 18 early genes. *Embo J*. 1986;5:2285-2292.
56. Spangle JM, Ghosh-Choudhury N, Munger K. Activation of cap-dependent translation by mucosal human papillomavirus E6 proteins is dependent on the integrity of the LXXLL binding motif. *J Virol*. 2012;86:7466-7472.
57. Seedorf K, Oltersdorf T, Krammer G, Rowekamp W. Identification of early proteins of the human papilloma viruses type 16 (HPV 16) and type 18 (HPV 18) in cervical carcinoma cells. *EMBO J*. 1987;6:139-144.
58. Yee C, Krishnan-Hewlett I, Baker CC, Schlegel R, Howley PM. Presence and expression of human papillomavirus sequences in human cervical carcinoma cell lines. *Am J Pathol*. 1985;119:361-366.
59. Crook T, Wrede D, Vousden KH. p53 point mutation in HPV negative human cervical carcinoma cell lines. *Oncogene*. 1991;6:873-875.
60. Lee AJ, Ashkar AA. The dual nature of type I and type II interferons. *Front Immunol*. 2018;9:2061.
61. Platanias LC. Mechanisms of type-I- and type-II-interferon-mediated signalling. *Nat Rev Immunol*. 2005;5:375-386.
62. Suk K, Chang I, Kim YH, et al. Interferon gamma (IFNgamma) and tumor necrosis factor alpha synergism in ME-180 cervical cancer cell apoptosis and necrosis. IFNgamma inhibits cytoprotective NF-kappa B through STAT1/IRF-1 pathways. *J Biol Chem*. 2001;276:13153-13159.
63. Chin YE, Kitagawa M, Kuida K, Flavell RA, Fu XY. Activation of the STAT signaling pathway can cause expression of caspase 1 and apoptosis. *Mol Cell Biol*. 1997;17:5328-5337.
64. White EA, Howley PM. Proteomic approaches to the study of papillomavirus-host interactions. *Virology*. 2013;435:57-69.
65. Neveu G, Cassonnet P, Vidalain P-O, et al. Comparative analysis of virus-host interactomes with a mammalian high-throughput protein complementation assay based on Gaussia princeps luciferase. *Methods*. 2012;58:349-359.
66. Ebner FA, Sailer C, Eichbichler D, et al. A ubiquitin variant-based affinity approach selectively identifies substrates of the ubiquitin ligase E6AP in complex with HPV-11 E6 or HPV-16 E6. *J Biol Chem*. 2020;295:15070-15082.
67. Mortensen F, Schneider D, Barbic T, et al. Role of ubiquitin and the HPV E6 oncoprotein in E6AP-mediated ubiquitination. *Proc Natl Acad Sci USA*. 2015;112:9872-9877.
68. Ronco LV, Karpova AY, Vidal M, Howley PM. Human papillomavirus 16 E6 oncoprotein binds to interferon regulatory factor-3 and inhibits its transcriptional activity. *Genes Dev*. 1998;12:2061-2072.
69. Li S, Labrecque S, Gauzzi MC, et al. The human papilloma virus (HPV)-18 E6 oncoprotein physically associates with Tyk2 and impairs Jak-STAT activation by interferon-alpha. *Oncogene*. 1999;18:5727-5737.

70. Pumroy RA, Cingolani G. Diversification of importin-alpha isoforms in cellular trafficking and disease states. *Biochem J*. 2015;466:13-28.
71. Frieman M, Yount B, Heise M, et al. Severe acute respiratory syndrome coronavirus ORF6 antagonizes STAT1 function by sequestering nuclear import factors on the rough endoplasmic reticulum/Golgi membrane. *J Virol*. 2007;81:9812-9824.
72. Du Y, Bi J, Liu J, et al. 3Cpro of foot-and-mouth disease virus antagonizes the interferon signaling pathway by blocking STAT1/STAT2 nuclear translocation. *J Virol*. 2014;88:4908-4920.
73. Wang R, Nan Y, Yu Y, Zhang YJ. Porcine reproductive and respiratory syndrome virus Nsp1beta inhibits interferon-activated JAK/STAT signal transduction by inducing karyopherin-alpha1 degradation. *J Virol*. 2013;87:5219-5228.

SUPPORTING INFORMATION

Additional supporting information may be found in the online version of the article at the publisher's website.

How to cite this article: Wang Y, Liu R, Liao J, et al. Orthogonal ubiquitin transfer reveals human papillomavirus E6 downregulates nuclear transport to disarm interferon-γ dependent apoptosis of cervical cancer cells. *FASEB J*. 2021;35:e21986. doi:10.1096/fj.202101232RR